

Straightforward differentiation of the viscous terms in Eq. (1) allows them to be written

$$\mu \left(\nabla^2 u_i + \frac{\partial \Delta / \partial x_i}{3} \right) + \frac{2(e_{ij} \partial \mu / \partial x_j - \Delta \partial \mu / \partial x_i)}{3} \quad (3)$$

In addition, the appropriate vector calculus identity allows this expression to be rewritten as

$$-\mu (\nabla \times \omega)_i + \frac{4}{3} \frac{\mu \partial \Delta}{\partial x_i} + 2 \left(e_{ij} \frac{\partial \mu}{\partial x_j} - \frac{\Delta \partial \mu}{\partial x_i} \right) \quad (4)$$

In order to derive the vorticity transport equation, this expression is substituted into the equations of motion, each term is divided by density ρ , and the entire expression is subjected to the curl operator. Comparing this with Eq. (1) in Ref. 1, it is clear that the additional variable viscosity terms

$$2 \nabla \times \frac{(e_{ij} \partial \mu / \partial x_j - \Delta \partial \mu / \partial x_i)}{\rho} \quad (5)$$

must be addressed for general viscous flows.

The focus of interest in this study is the effect of the first term in flows for which the approximation $\rho \approx \text{constant}$, $\Delta \approx 0$ is a good one, yet μ must be allowed to vary. In addition to various laminar flows, this situation is applicable to turbulence modeling as well, in which μ is related to the local flowfield properties. We consider, therefore, the following term in the general vorticity transport balance:

$$\left(\frac{2}{\rho} \right) \nabla \times \left(e_{ij} \frac{\partial \mu}{\partial x_j} \right) \quad (6)$$

For cases of interest in which μ varies predominantly in one direction, herein x_2 , the components of the curl in the three orthogonal directions are

$$\begin{aligned} \frac{\partial}{\partial x_2} \left(e_{32} \frac{\partial \mu}{\partial x_2} \right) - \frac{\partial}{\partial x_3} \left(e_{22} \frac{\partial \mu}{\partial x_2} \right); & \quad x_1 \\ \frac{\partial}{\partial x_1} \left(e_{32} \frac{\partial \mu}{\partial x_2} \right) - \frac{\partial}{\partial x_3} \left(e_{12} \frac{\partial \mu}{\partial x_2} \right); & \quad x_2 \\ \frac{\partial}{\partial x_1} \left(e_{22} \frac{\partial \mu}{\partial x_2} \right) - \frac{\partial}{\partial x_2} \left(e_{12} \frac{\partial \mu}{\partial x_2} \right); & \quad x_3 \end{aligned} \quad (7)$$

If x_1 , x_2 , and x_3 are associated with the streamwise, normal, and spanwise coordinates of a shear flow, it is clear that explicit three-dimensionality is required to impact streamwise vorticity from variable viscosity terms. However, in two-dimensional flow, the spanwise vorticity is affected by the component of the curl in x_3 :

$$\frac{\partial \mu}{\partial x_2} \left(\frac{\partial e_{22}}{\partial x_1} - \frac{\partial e_{12}}{\partial x_2} \right) - \frac{\partial^2 \mu}{\partial x_2^2} e_{12} \quad (8)$$

which may be written

$$\frac{\partial \mu}{\partial x_2} \left(\frac{\partial}{\partial x_2} \frac{\omega_3}{2} \right) - \frac{\partial^2 \mu}{\partial x_2^2} e_{12} \quad (9)$$

If, in addition, $u_2 \ll u_1$, this expression further reduces to one-half of

$$\frac{\partial \mu}{\partial x_2} \left(\frac{\partial}{\partial x_2} \frac{\partial u_1}{\partial x_2} \right) - \frac{\partial^2 \mu}{\partial x_2^2} \frac{\partial u_1}{\partial x_2} \quad (10)$$

or

$$\frac{\partial \mu}{\partial x_2} \frac{\partial^2 u_1}{\partial x_2^2} - \frac{\partial^2 \mu}{\partial x_2^2} \frac{\partial u_1}{\partial x_2} \quad (11)$$

If, for example, μ exhibits some empirical dependence on, say, $\partial u_1 / \partial x_2$, the vorticity generation will respond to a term proportional to

$$\mu \frac{\partial^2 \mu}{\partial x_2^2} - \left(\frac{\partial \mu}{\partial x_2} \right)^2 \quad (12)$$

which, clearly, can undergo several sign changes across a shear flow and contribute positive or negative terms to the vorticity balance. The accurate representation of variable viscosity effects is, therefore, critical in representing the detailed vortical mechanics.

Acknowledgment

This work was carried out under the sponsorship of the Aerospace Sciences Directorate, Air Force Office of Scientific Research.

References

- ¹Lakshminarayana, B. and Horlock, J. H., "Generalized Expressions for Secondary Vorticity Using Intrinsic Co-ordinates," *Journal of Fluid Mechanics*, Vol. 59, Pt. 1, 1973, pp. 97-115.
- ²Batchelor, G. K., *An Introduction to Fluid Dynamics*, Cambridge University Press, 1970, p. 147.

Triple-Velocity Products in a Channel with a Backward-Facing Step

R. S. Amano* and P. Goelt†

University of Wisconsin, Milwaukee, Wisconsin

Introduction

PREDICTING physical behavior of separating and recirculating flows is an important aspect in aeronautics and in many industrial problems. To improve turbulence modeling for such complex turbulent flows, it is necessary to conduct an extensive study of turbulence behavior in reattaching shear flows.

Experimental observations by Chandrsuda and Bradshaw¹ show that when the separated flow reattaches on a solid wall, the separated mixing layer begins to change rapidly, and large-scale eddies are suppressed due to the solid wall, leading to a marked decrease in the triple-velocity products of turbulence fluctuating velocities toward the solid surface from the region of maximum turbulence intensity.

This paper focuses on the evaluation of the triple-velocity products in the reattaching and redeveloping region behind a step. As discussed above, the change in triple-velocity products is significant in the wake region, resulting in a considerable variation in the diffusion rate of the Reynolds stresses. Thus, it is important to reevaluate the existing models of the third-order closure for better understanding of such diffusion processes in the separated shear layers. In the present paper four models of the third-order closure are examined, and the results are compared with the experimental data of Chandrsuda and Bradshaw.¹ The models considered are those proposed by Daly and Harlow,² Hanjalic and Launder,³ Shir,⁴ and Cormack et al.⁵

Submitted July 22, 1985; revision received Sept. 3, 1985. Copyright © American Institute of Aeronautics and Astronautics, Inc., 1985. All rights reserved.

*Associate Professor, Department of Mechanical Engineering.

†Research Assistant, Department of Mechanical Engineering.

Third-Order Closure Models

The set of differential equations governing the transport of the kinematic Reynolds stresses $-u_i u_j$ can be written in the form

$$\begin{aligned} (U_k \overline{u_i u_j})_{,k} = & -(\overline{u_j u_k} U_{i,k} + \overline{u_i u_k} U_{j,k}) - 2\nu \overline{u_{i,k} u_{j,k}} \\ & + (p/\rho) (\overline{u_{i,j} + u_{j,i}}) - [\overline{u_i u_j u_k} - \nu (\overline{u_i u_j})_{,k} \\ & + (p/\rho) (\delta_{jk} \overline{u_i} + \delta_{ik} \overline{u_j})]_{,k} \end{aligned} \quad (1)$$

where U and u represent mean and fluctuating velocities, respectively, and p shows fluctuating pressure.

Attention is focused primarily on the triple-velocity products—the first term inside the last bracket on the right-hand side of Eq. (1), since the rest of the terms in that bracket are insignificant compared with the first term. Algebraic correlations for the triple-velocity products have been proposed by several researchers; all of them are tested for parabolic shear flows such as boundary layers, jets, wakes, and duct flows. In the present paper four models are considered and tested for the reattaching shear flows, including flow recirculation near the step. These models are as follows:

1) The model of Daly and Harlow²

$$\overline{u_i u_j u_k} = -0.25 C_p (k/\epsilon) \overline{u_k u_i} (\overline{u_i u_j})_{,l} \quad (2)$$

2) The model of Hanjalic and Launder³

$$\begin{aligned} \overline{u_i u_j u_k} = & -0.11 C_p (k/\epsilon) [\overline{u_i u_j} (\overline{u_i u_k})_{,l} + \overline{u_i u_l} (\overline{u_j u_k})_{,l} \\ & + \overline{u_l u_k} (\overline{u_i u_j})_{,l}] \end{aligned} \quad (3)$$

3) The model of Shir⁴

$$\overline{u_i u_j u_k} = -0.04 C_p (k^2/\epsilon) (\overline{u_i u_j})_{,k} \quad (4)$$

4) The model of Cormack et al.⁵

$$\begin{aligned} \overline{u_i u_j u_k} = & C_p \left[4 \frac{k^2}{\epsilon} \{ 2\alpha_1 (\delta_{ij} \delta_{kl} + \delta_{ik} \delta_{jl} + \delta_{kj} \delta_{il}) k_{,l} \right. \\ & + \alpha_2 (a_{ik,j} + a_{ij,k} + a_{kj,i}) \} \\ & + 2 \frac{k}{\epsilon} \{ 2\alpha_3 (\delta_{ik} a_{jl} + \delta_{ij} a_{kl} + \delta_{jk} a_{il}) k_{,l} \\ & \left. + \alpha_4 (a_{ik} a_{jl} + a_{ij} a_{kl} + a_{kj} a_{il}) \} \right] \end{aligned} \quad (5)$$

where

$$a_{ij} = \overline{u_i u_j} - (2/3) \delta_{ij} k \quad (6)$$

and the values for α_i are given in Table 1.

The coefficient C_p appearing in Eqs. (2-5) is unity in the original forms. Upon comparison with the experimental data for a separating and reattaching flow beyond a step, the value of C_p had to be modified in order that the computed levels of $\overline{u_i u_j u_k}$ agree with the experimental data. The recommended values for C_p are given in the next section.

Results and Discussion

Before computing triple-velocity products in the region behind a step, each component of the Reynolds stress equation (1) was solved along with the momentum, turbulence energy, and turbulence energy dissipation rate equations. The method for solving these equations is similar to that used in Ref. 6, which may be referred to for a detailed description.

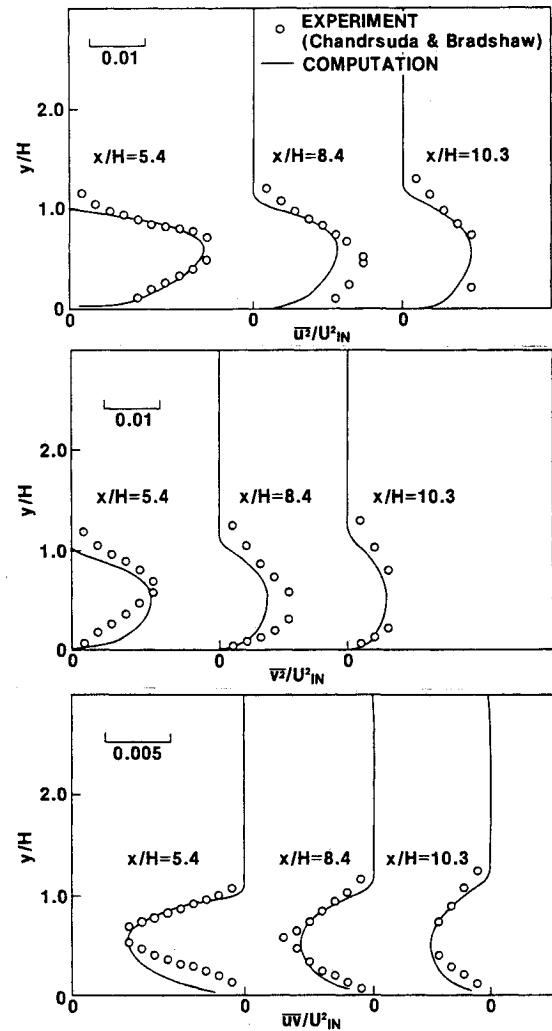


Fig. 1 Reynolds-stress profiles beyond the step.

Table 1 Values for α_i

α_1	α_2	α_3	α_4
-9.14×10^{-3}	-1.72×10^{-2}	-4.80×10^{-2}	-1.02×10^{-1}

To establish an optimum grid system, exploratory grid tests were performed using 32×32 , 42×42 , and 52×52 mesh sizes and several different grid expanding factors in the downstream direction. Because computations with coarse mesh sizes fail to provide a decipherable trend in the Reynolds stress distributions, the mesh size of 52×52 was used with an axial length of 50 step heights for a step ratio of $Y_0/H=2.5$. The grid expansion factors used in the streamwise and transverse directions were 1.01 and 1.02, respectively.

Figure 1 shows the normal Reynolds stresses ($\overline{u^2}$ and $\overline{v^2}$) and the shear Reynolds stress (\overline{uv}) distributions at three different locations in the flowfield beyond a step. As shown in Fig. 1, all the Reynolds stresses decay in the region downstream of the reattachment. In general, agreement between the computed results and the experimental data of Chandrsuda and Bradshaw¹ is fairly good. Based on this agreement with the experimental data, the values of these Reynolds stresses were used to evaluate the algebraic models of the triple-velocity correlations [Eqs. (2-5)].

Figure 2 represents the distribution of the triple-velocity products at four different locations in the reattaching shear layer. It is commonly observed that all the models under-

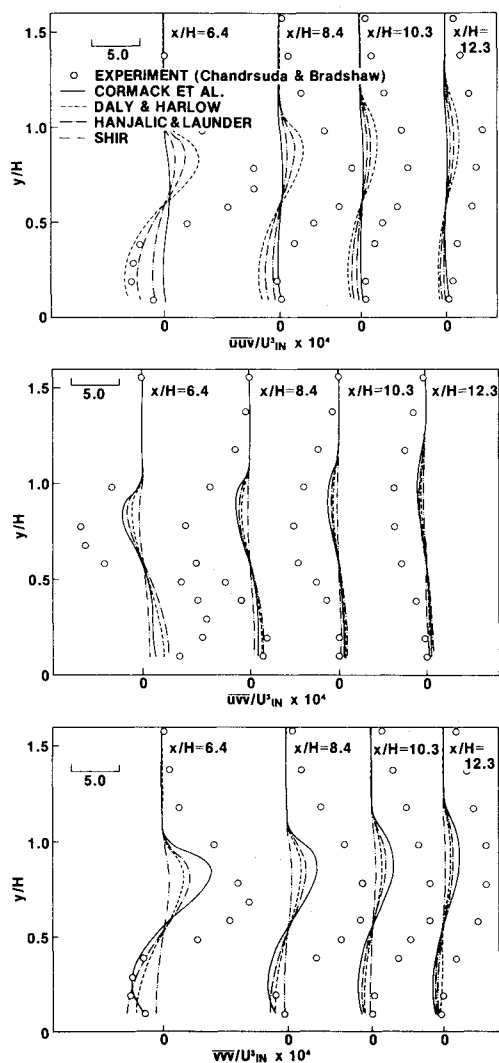


Fig. 2 Triple-velocity product profiles beyond the step (original models).

predict the levels of triple-velocity products everywhere. While the model of Shir consistently gives low levels, the model of Cormack et al. gives the highest levels for uuv and vvv . The model of Daly-Harlow, which is most frequently used, gives relatively lower levels except for uuv , whereas the model of Hanjalic-Launder is more acceptable because it gives reasonably high levels for every component of the triple-velocity products.

In order to adjust for the discrepancy in the peak values of the triple-velocity products, the multiplying factor C_p in Eqs. (2-5) was incorporated to compensate suitably for the difference in the levels. This was done by dividing the experimental peak values of $u_i u_j u_k$ by those predicted by the particular algebraic model. These factors were obtained for uuv , uvv , and vvv profiles at x/H locations of 6.4, 8.4, 10.3, and 12.3 for all four algebraic models.

Table 2 shows the values of these factors for individual components and models. The overall factor for a particular model is then obtained by averaging all the values of C_p for all the components of $u_i u_j u_k$ for that model.

The triple-velocity products were recomputed by using the overall averaged factors, and the results are shown in Fig. 3. It is interesting to note that the peak values obtained by using the model of Hanjalic-Launder agree with the experimental data for all the components, whereas those obtained by other models agree with the experimental data only for uuv component. This indicates that, although the levels of the triple-velocity products can easily be adjusted according to flow conditions, we cannot necessarily obtain universally im-

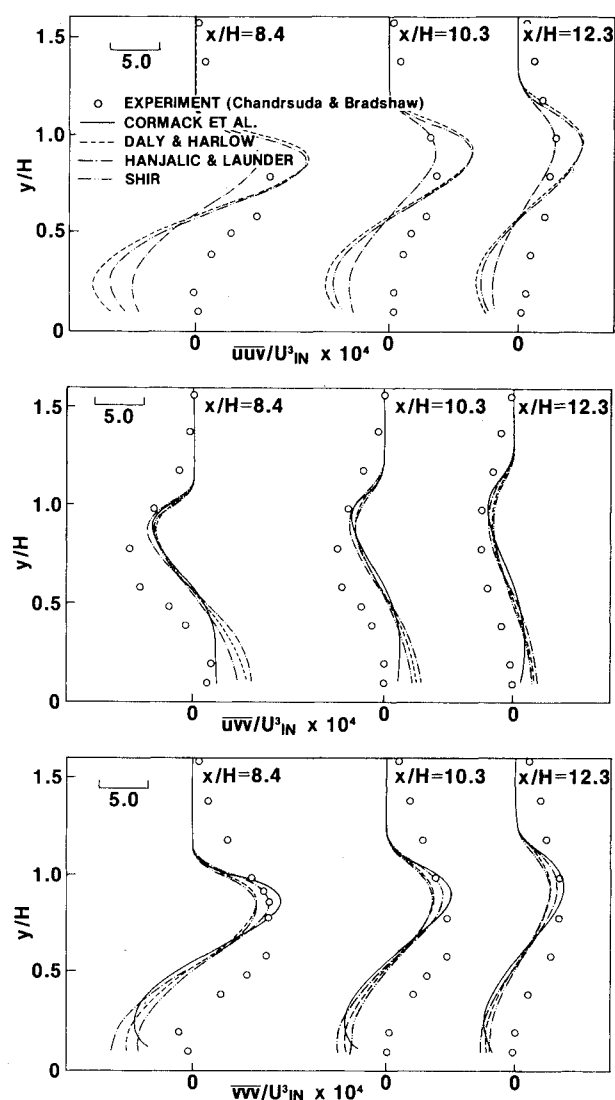


Fig. 3 Triple-velocity product profiles beyond the step (overall correction factors are used).

Table 2 Correction factors for $u_i u_j u_k$ for different algebraic models

C_p				
Models	uuv	uvv	vvv	Overall average
Daly-Harlow	2.66	4.93	6.45	4.68
Hanjalic-Launder	4.18	3.74	4.76	4.22
Shir	7.68	14.20	18.66	13.51
Cormack et al.	—	2.12	3.52	2.82

proved results for every component of $u_i u_j u_k$ when using models other than that of Hanjalic-Launder.

The reason the model of Hanjalic-Launder gives better results for all the components of $u_i u_j u_k$ is that in the derivation process of this model the generation rates due to turbulence stresses as well as the diffusion rates of $u_i u_j u_k$ were taken into account, although the convection and the generation rates due to mean strains were neglected (see Ref. 3). The generation caused by the stresses is particularly significant in the reattaching shear layer.

Unlike this model, the models of Daly-Harlow and Shir do not include nonhomogeneous flow effects. That is, when the Shir model, for example, is used, the transverse gradient of u^2 is the only component that evaluates the behavior of the triple-velocity product uuv in the transport equation of u^2 . The model of Daly-Harlow has an additional component

that accounts for the variation of $\overline{u^2}$ in the streamwise direction for the corresponding product. However, these two models are notably limited in comparison with the Hanjalic-Lauder model, which accounts for variations of the shear stress in both directions in addition to the $\overline{u^2}$ variations. It should, however, be noted that all the models would produce similar results in an isotropic turbulence flowfield.

The model of Cormack et al. was evaluated only for uvu and uvv since the values computed for uvu using its original form were not high enough to estimate the factor C_p within a reasonable range (see Fig. 2). Otherwise, the values of C_p derived using the model of Cormack et al. were the lowest, indicating that this model gives the best agreement with experiments when used in its original form.

Conclusions

1) The triple-velocity products need to be predicted accurately in the reattaching shear layer in order to evaluate appropriately the diffusion process of the Reynolds stress. The behavior of the triple-velocity products in such a complex turbulent flow is different from that in simpler flows.

2) All the existing algebraic models for the triple-velocity products underpredict the levels of $u_i u_j u_k$ in the reattaching shear layer. The predicted levels can easily be improved by using a correction factor.

3) With the exception of the model of Hanjalic-Lauder, all models cannot be improved simply by employing a single value for C_p . Thus, it is difficult to obtain a unique value for the correction factor. This is because the Hanjalic-Lauder model is the only one that includes the generation terms due to Reynolds stresses.

Finally, it was observed that none of the above models accurately predict the overall levels of the triple-velocity products, primarily because the convection effect of the triple-velocity products is never considered at all. This effect may be small in simple shear layers but is significantly large when the shear layer reattaches on a solid wall, creating high turbulence energy near the wall and, subsequently, these high levels are transported in the downstream direction. In consequence, a transport model for $u_i u_j u_k$ that takes this process into account must be developed and tested for complex turbulent flows.

Acknowledgment

This work was sponsored by NASA Lewis Research Center under Grant NAG 3-546 monitored by Mr. Thomas VanOberbeke.

References

- ¹Chandrsuda, C. and Bradshaw, P., "Turbulence Structure of a Reattaching Mixing Layer," *Journal of Fluid Mechanics*, Vol. 110, 1980, pp. 171-194.
- ²Daly, B. J. and Harlow, F. H., "Transport Equations in Turbulence," *Physics of Fluids*, Vol. 13, No. 11, 1970, pp. 2634-2649.
- ³Hanjalic, K. and Launder, B. E., "A Reynolds Stress Model of Turbulence and Its Application to Thin Shear Flows," *Journal of Fluid Mechanics*, Vol. 52, Pt. 4, 1972, pp. 609-638.
- ⁴Shir, C. C., "A Preliminary Numerical Study of Atmospheric Turbulent Flows in the Idealized Planetary Boundary Layer," *Journal of Atmospheric Science*, Vol. 30, Oct. 1973, pp. 1327-1339.
- ⁵Cormack, D. E., Leal, L. G., and Seinfeld, J. H., "An Evaluation of Mean Reynolds Stress Turbulence Models: The Triple-Velocity Correlation," *ASME Journal of Fluids Engineering*, Vol. 100, March 1978, pp. 47-54.
- ⁶Amano, R. S. and Goel, P., "Computations of Turbulent Flow Beyond Backward-Facing Steps by Using Reynolds-Stress Closure," *AIAA Journal*, Vol. 23, Sept. 1985, pp. 1356-1361.

Numerical Evaluation of Propeller Noise Including Nonlinear Effects

K. D. Korkan* and E. von Lavante†

Texas A&M University, College Station, Texas
and

L. J. Bober‡

NASA Lewis Research Center, Cleveland, Ohio

Introduction

THE continued pressure on aircraft manufacturers by communities and regulatory agencies to reduce noise levels requires a thorough analysis of the characteristics of the acoustic field induced by the propulsion unit. To this end, the accurate determination of noise levels generated specifically by propellers has been the subject of numerous experimental and theoretical studies. Recent studies have utilized the Ffowkes Williams-Hawkings formulation,¹ an extension of Lighthill's theory,^{2,3} to make significant contributions to the theory and numerical computation of helicopter rotor and propeller noise.⁴ However, the linear character of the present acoustic calculations still does not account for the quadrupole noise term, but does give reasonable correspondence with experiment up to transonic tip speeds. In the present study, the propeller noise in the acoustic near field is determined by integration of the pressure-time history in the tangential direction of a numerically generated flowfield about the SR-3 propfan, including the shock wave system in the vicinity of the propeller tip. As a result, the quadrupole source terms are accounted for in the present acoustic analysis, which yields overall sound pressure levels and the associated frequency spectra as a function of observer location.

Prediction of the Transonic Flowfield

The propfan configuration used in this analysis is an eight-blade SR-3 series propeller with a radius of 12.25 in. and blade angle at three-quarter radius of 61.3 deg. The analysis was applied to this configuration operating at several different freestream Mach numbers. The helical tip Mach numbers, advance ratios, rotational velocities, and power coefficients are shown in Table 1.

The transonic flowfield around the SR-3 propeller and axisymmetric spinner/nacelle configuration was computed using the NASPROP-E computer code developed by Bober et al.⁵ The governing three-dimensional Euler equations are formulated in weak conservation law form, subject to transformation into body-fitted general coordinates. These equations correctly describe most of the physical phenomena, including nonlinear effects such as the propeller tip shock wave system. The equations were solved in the blade-to-blade physical domain using an implicit finite difference approximate factorization scheme. Since central differencing was applied, it was necessary to add numerical damping to assure stable time marching. It is assumed that the periodicity of the flow limits the size of the computational domain to the region between two adjacent blades. Typically, the solution method used 45 points in the axial direction, 21 points in the radial direction, and 11 points in the circumferential

Received April 22, 1985; revision received Aug. 12, 1985.
Copyright © American Institute of Aeronautics and Astronautics, Inc., 1985. All rights reserved.

*Associate Professor, Aerospace Engineering Department, Associate Fellow AIAA.

†Assistant Professor, Aerospace Engineering Department, Member AIAA.

‡Head, Propeller Aerodynamics Section. Member AIAA.